ALCOA

ALCOA RESEARCH LABORATORIES

2 of 3

602120

INVESTIGATION OF THE MECHANISM OF STRESS CORROSION OF ALUMINUM ALLOYS

Bureau of Naval Weapons Contract NOw64-0170c

45 pp #1.25

Second Quarter Report

(Period of March 1, 1964 to May 31, 1964)

Reported by: G. C. English ENH

G. C. English

William King

Approved by: E H Hollingsworth

E. H. Hollingsworth

July 6, 1964

TABLE OF CONTENTS

SYNOPSIS

In the second quarter, cathodic protection studies on the samples of 2024 and 7075 alloy plate prepared to represent a range of susceptibility to stress corrosion were continued; the new anodic polarization technique described earlier was investigated further; the samples were examined metallographically with the electron microscope using the thin foil transmission technique and with the light microscope; and magnetic susceptibility measurements were made.

The electron microscopic examinations emphasize the complexity of the structures of both 2024 and 7075 alloys. They also emphasize the difficulty involved in isolating and reproducing even the simplest features of these structures. Features ranging from an initial clustering of atoms to the formation of final equilibrium precipitate are evident. Electrical conductivity and magnetic susceptibility measurements were investigated for following the development of these features. The evidence suggests that magnetic susceptibility may indicate a somewhat earlier stage of solid solution decomposition than electrical conductivity.

Some of the difficulties anticipated in the cathodic protection studies have been encountered. The corrosion of specimens in salt solution under conditions of total immersion is much too slow to permit convenient establishment of cathodic protection. More corrosive solutions will be required. Also, it may be necessary to use specimens taken in a more susceptible direction.

INTRODUCTION:

This report summarizes work during the period of March 1, 1964 to May 31, 1964. In this period, 625.5 man hours were spent on the contract. The work consisted of a continuation of the cathodic protection studies and the anodic polarization measurements described earlier; an evaluation of the stress corrosion performance of the various samples of 2024 and 7075 alloy plate that were prepared to reflect a range of susceptibility to stress corrosion; a metallographic examination of these samples with the electron microscope using the thin foil transmission technique and with the light microscope; and finally, the measurement of magnetic susceptibility and electrical conductivity.

MATERIALS:

Samples of the 1/4-inch thick 2024-F and 7075-F alloy plate from regular plant production were solution heat-treated in the laboratory and quenched in cold water or in boiling water. Samples with each type of quench were then naturally or artificially aged to produce 2024-T4 and -T6 and 7075-W, -T6, and -T73.

The results of tensile tests and of standard stress corrosion tests by alternate immersion in 3-1/2% NaCl solution are summarized in Table I. As is evident, none of the specimens have failed in the alternate immersion test at the end of eight weeks. Previous work suggests that some of these specimens will fail before completion of the 12-week test period normally used. Specimens that do not fail during the total test period will be compared on the basis of the loss in tensile strength.

There is little question that these materials reflect the wide range in resistance to stress corrosion desired even though this range has not been detected in the standard corrosion test. Practical experience with standard products in tempers represented by the samples demonstrates this point as do the metallographic examinations and electrical conductivity measurements made upon the samples.

CATHODIC PROTECTION STUDIES:

Cathodic protection was proposed as a method for establishing the potential of the most anodic region in a corroding specimen. In theory, cathodic protection is complete when a specimen is cathodically polarized to a potential equal to that of the most anodic region. At this potential, electrochemical corrosion should cease.

Tests were made on both unstressed and stressed sub-size tensile specimens immersed in 1 N sodium chloride adjusted to pH 4 and pH 10. The course of corrosion was then followed by measurement of electrical conductivity as described earlier.

Unfortunately, the rate of corrosion in the solutions selected was so slow that it was difficult to determine the minimum potential required for complete protection. For example, specimens changed only 3% in electrical conductivity after exposure for 30 days in 1 N sodium chloride solution at pH 4.

This rather slow rate of corrosion reflects several conditions. It reflects the fact that specimens were exposed by total immersion rather than by alternate immersion which accelerates attack. It reflects the fact that specimens were taken in the long transverse direction rather than in the more susceptible short

transverse direction. Finally, it reflects the fact that the solutions themselves were not inherently corrosive enough.

METALLOGRAPHIC EXAMINATIONS

Electron micrographs illustrating the structures of the four samples of 2024 alloy plate and the six samples of 7075 alloy plate are presented in Figures 1 - 10. The structures are described in considerable detail in the captions of these figures. Figures 11 - 12 are conventional light micrographs at 500X.

These micrographs provide a striking illustration of the complexity of the structures of 2024 and 7075 alloys. They also emphasize the difficulty that will be involved in isolating and reproducing any features of the structures to provide a simplified electrochemical model, as proposed in the contract. Certainly, the initial work in this direction should be restricted to the simplest structures. With little question, these structures are found in the as-quenched samples. The structure of a cold water quenched sample approaches most closely that of an ideal, single phase solid solution. The structure of a boiling water quenched sample contains considerable precipitate. But, this precipitate, by far and large, is in an advanced stage. For the most part, intermediate transition precipitate and still earlier stages of its formation, such as zones, are missing, or at least, present in relatively small amounts. As artificial aging proceeds, the structure tends to become more and more complex reflecting the development of larger amounts of zones and transition precipitate

Some attention, perhaps, should be given to differences in the structures of 2024 and 7075 alloys. The most obvious difference is the greater tendency for precipitate formation with decreasing quenching rate in 7075 than in 2024 alloy. This greater quench sensitivity of 7075 alloy is well known. Nonetheless, the electron micrographs illustrate the difference very well. Another important difference is the much greater tendency for 7075 alloy to form zones. The most obvious difference between the -T6 and -T73 tempers of 7075 alloy is in the number and size of these zones; this difference is reflected in a substantial difference in stress corrosion performance.

MAGNETIC SUSCEPTIBILITY MEASUREMENTS

Magnetic susceptibility measurements are summarized in Table II together with electrical conductivity measurements for comparison. This comparison is shown more clearly in Figure 13.

In the proposal, the possibility of utilizing some of the newer tools for evaluating metallurgical structure was suggested. One of these tools is magnetic susceptibility. The significance of the magnetic susceptibility of aluminum alloys is still being explored. In many respects, magnetic susceptibility is comparable to electrical conductivity. Like electrical conductivity, it is sensitive to phase changes, and it can be used to follow the decomposition of a solid solution in aluminum alloys. When solute atoms are precipitated, more conduction electrons become available, and the greater availability of these electrons results in an increase in both conductivity and magnetic susceptibility. On the other hand, magnetic susceptibility, unlike electrical conductivity, is not affected by factors such as residual

or applied stress.

As plotted in Figure 13, the data for both alloys suggest a direct, or nearly direct, proportionality between electrical conductivity and magnetic susceptibility for samples quenched at the same rate. Within the limits of experimental error, the data for 2024 alloy could have been plotted without showing an effect of quenching rate. There is some question, therefore, whether the relationship between electrical conductivity and magnetic susceptibility for the two alloys differs in degree or in kind.

A direct proportionality suggests, of course, that the two factors are affected by, or sensitive to, the same structural conditions that result from decomposition of a solid solution. On the other hand, the two curves for each alloy representing the two quenching rates suggests the introduction during quenching of some structural condition that affects the two measurements differently. It is informative to consider briefly what this condition might be even though it is to be emphasized that the limited data available by no means provide conclusive evidence for it. One possibility is that the difference is related to zone formation. The simplest argument that can be proposed is that both electrical conductivity and magnetic susceptibility reflect the formation of precipitate, but that only magnetic susceptibility reflects zone formation. Alternatively, it can be argued that zone formation leads to an increase in both conductivity and susceptibility, but that the increase in conductivity is, at least partly cancelled because of the effects of lattice strains associated with zone formation.

Some evidence for these possibilities is provided by the fact that zone formation is more pronounced in 7075 alloy than in 2024 alloy. This difference is in agreement with the fact that the curves for 7075 alloy are displaced to a significant degree while those for 2024 alloy are displaced to only a negligible degree although they are displaced in the proper direction. Further evidence will require a more thorough examination at higher magnification to resolve zone formation more clearly than in the micrographs in Figures 1 - 10.

ANODIC POLARIZATION STUDIES:

Anodic polarization curves for the four samples of 2024 alloy and for the six samples of 7075 alloy in 1 N sodium chloride solution adjusted to pH 4 are shown in Figures 14-16. These curves were established with the scanning technique described earlier. They provide further evidence of the correlation of anodic polarization behavior to stress corrosion performance. Again, the current density at the intersection of the two branches of each curve appears to be a measure of susceptibility to intergranular attack as does the area between the lower branch and the potential axis.

Attention should again be called to the fact that the potential level of the upper branch of each curve appears to reflect the amount of alloying elements in solid solution as does the conventional solution potential.

FUTURE WORK:

Major attention is being devoted to finding an electrolyte that produces much faster corrosion than the electrolytes used so far. Possibilities include sodium chloride solutions of still lower pH, sodium chloride solutions containing too little anodic inhibitor, sodium chloride solutions containing heavy metal contamination, and electrolytes such as methyl alcohol and carbon tetrachloride. The anodic polarization technique will be used to evaluate these solutions as thoroughly as possible because this technique is somewhat faster than cathodic protection studies. For some phases of the work, thicker plate that permits short transverse specimens will be obtained and used to speed up stress-corrosion cracking.

At this stage, it also seems well to restrict the overall endeavor somewhat. Some selection will be made of tempers to reflect good and poor performance with regard to stress corrosion. This selection will be restricted to the simplest microstructures possible.

There is no certainty that the cathodic protection studies will provide enough information about phases in time to assist in the preparation of these phases. It turns out, however, that a great deal of information about these phases is available from the literature and from work at these Laboratories. It seems desirable, therefore, to start the preparation of phases almost immediately rather than to wait further. Hopefully, some of these phases can be used to represent at least the simpler possible structures.

Distribution List for Contract NOw 64-0170-c

1. Bureau of Naval Weapons
   Department of the Navy
   Washington 25, D. C.
   Internal distribution to be made by DLI-3 as follows:
   RRMA-222 (3 copies plus remainder after distribution)
   RRMA-5

2. Defense Documentation Center for Scientific & Technical Information(DDC)
   Arlington Hall Station
   Arlington 12, Virginia
   Attn: Document Service Center (TICSP) - (12 copies) (with a note stating "No Restrictions for DDC Distribution)

3. Bureau of Ships
   Department of the Navy
   Washington 25, D. C.
   Attn: Code 342B

4. Office of Naval Research
   Department of the Navy
   Washington 25, D. C.
   Attn: Code 423

5. Naval Air Material Center
   Aeronautical Materials Laboratory
   Philadelphia 12, Pennsylvania

6. Air Force Materials Laboratory
   Research & Technology Division
   Wright Patterson Air Force Base
   Ohio 45433
   Attn: MAMD
   MAAE

7. National Aeronautics & Space Administration
   Federal Building #10
   Washington, D. C. 20546
   Attn: Code RRM

8. Technical Information Service Extension
   U. S. Atomic Energy Commission
   P. O. Box 62
   Oak Ridge, Tennessee

9. Director
   National Bureau of Standards
   Washington 25, D. C.

10. Commanding Officer
    Office of Ordnance Research
    Box CM, Duke Station
    Durham, North Carolina

Distribution List (continued) NOw 64-0170-c

11. Army Materials Research Agency
Watertown Arsenal
Watertown, Massachusetts

12. U. S. Atomic Energy Commission
Document Library
Germantown, Maryland

13. Battelle Memorial Institute
505 King Avenue
Columbus 1, Ohio

14. U. S. Naval Research Laboratory
Washington 25, D. C.

15. U. S. Naval Ordnance Laboratory
White Oak, Silver Spring, Maryland
Attn: WM Division

16. Dow Metal Products Company
Midland, Michigan

17. Missile & Space Flight Center
P. & V. E. Labs.
Huntsville, Alabama
Attn: Mr. J. G. Williamson

18. Kaiser Aluminum & Chemical Corp.
Dept. of Metallurgical Research
Spokone, Washington 99215
Attn: Mr. T. R. Pritchett

19. Reynolds Metals Company
6601 West Broad Street
Reynolds Building
Richmond 18, Virginia
Attn: Mr. Harry Jackson (MRL)

20. IIT Research Institute
Metals Research Dept.
10 West 35th Street
Chicago, Illinois 60616
Attn: Dr. F. A. Crossley

21. Mr. Abner R. Willmer
Chief of Metals Research
David Taylor Model Basin
Washington 7, D. C.

22. Commanding Officer
Frankford Arsenal
Philadelphia, Pennsylvania
Attn: Mr. H. Markus
1320 Bldg. 64-4.

TABLE I

STANDARD EVALUATION OF SAMPLES

S. No.	Alloy	Temper	Quench	Tensile Properties Longitudinal T.S. ksi	Y.S. ksi	El % in 4D	Transverse T.S. ksi	Y.S. ksi	El % in 4D	El Cc %
[illegible]	7075	-W	Cold Water	77.0	51.7	20.0	76.9	50.4	20.0	
[illegible]	7075	-W	Boiling Water	68.0	40.3	18.0	70.0	41.0	18.0	
[illegible]	7075	-T6	Cold Water	85.0	76.5	14.0	83.9	73.2	14.7	
[illegible]	7075	-T6	Boiling Water	67.0	49.6	16.0	68.4	49.7	15.3	
[illegible]	7075	-T73	Cold Water	76.2	67.7	14.0	77.3	68.3	12.0	
[illegible]	7075	-T73	Boiling Water	63.5	49.1	14.0	64.0	48.4	13.3	
[illegible]	2024	-T4	Cold Water	71.8	45.8	22.0	70.0	44.6	22.3	
[illegible]	2024	-T4	Boiling Water	68.1	41.8	20.0	68.3	41.6	20.0	
[illegible]	2024	-T6	Cold Water	69.7	56.5	12.7	69.3	56.1	12.0	
[illegible]	2024	-T6	Boiling Water	65.7	50.2	13.3	65.8	50.0	12.3	

Notes: (1) 6 Hour Exposure to 53 g/l NaCl + 9 c
I - intergranular; UP - undermining p

(2) Number of specimens that failed/numbe

TABLE I

D EVALUATION OF SAMPLES

ties Transverse			Electrical	Microscopic	3-1/2% NaCl Sol'n by Alternate Imm.			
				Examination	Stressed 75% Y.S.		Stressed 90% Y.S.	
S. ksi	Y.S. ksi	El % in 4D	Conductivity % I.A.C.S.	Type of Attack(1)	F/N (2)	Time	F/N (2)	Time
.9	50.4	20.0	27.8	P + SI	0/2	8 wks	0/2	8 wks
.0	41.0	18.0	33.3	I	0/2	8 wks	0/2	8 wks
.9	73.2	14.7	31.3	UP	0/2	8 wks	0/2	8 wks
.4	49.7	15.3	35.5	I	0/2	8 wks	0/2	8 wks
.3	68.3	12.0	39.0	P	0/2	8 wks	0/2	8 wks
.0	48.4	13.3	41.8	P	0/2	8 wks	0/3	8 wks
.0	44.6	22.3	28.8	I + P	0/2	8 wks	0/2	8 wks
.3	41.6	20.0	31.2	I	0/2	8 wks	0/2	8 wks
.3	56.1	12.0	36.1	I	0/2	8 wks	0/2	8 wks
.2	50.0	12.3	35.8	I + P	0/2	8 wks	0/2	8 wks

osure to 53 g/l NaCl + 9 cc H_2O_2 (P - pitting; SI - slight intergranular; anular; UP - undermining pitting.

pecimens that failed/number of specimens exposed.

TABLE II

RESULTS OF MAGNETIC SUSCEPTIBILITY M

S.No.	Alloy	Temper	Quench	Magnetic Susceptibility X10^6
306962	7075	W	C.W.Q.	0.4252
306963	7075	W	B.W.Q.	0.4449
306903	7075	-T6	C.W.Q.	0.4566
306904	7075	-T6	B.W.Q.	0.4539
306905	7075	-T73	C.W.Q.	0.5115
306906	7075	-T73	B.W.Q.	0.5184
306964	2024	-T4	C.W.Q.	0.4961
306965	2024	-T4	B.W.Q.	0.5095
306966	2024	-T6	C.W.Q.	0.5504
306967	2024	-T6	B.W.Q.	0.5482

Note: (1) CGS magnetic units.

TABLE II

ULTS OF MAGNETIC SUSCEPTIBILITY MEASUREMENTS

Quench	Magnetic Susceptibility $X10^6$ (1)	Electrical Conductivity % IACS
C.W.Q.	0.4252	27.8
B.W.Q.	0.4449	33.3
C.W.Q.	0.4566	31.3
B.W.Q.	0.4539	35.5
C.W.Q.	0.5115	39.0
B.W.Q.	0.5184	41.8
C.W.Q.	0.4961	28.8
B.W.Q.	0.5095	31.2
C.W.Q.	0.5504	36.1
B.W.Q.	0.5482	25.8

CGS magnetic units.

Figure 1

THIN FOIL TRANSMISSION ELECTRON MICROGRAPH
OF COLD WATER QUENCHED 2024-T4 ALLOY

The numerous particles are dispersoid of an Al-Cu-Mn phase that is substantially insoluble at the solution heat-treating temperature. No precipitate of a soluble, age hardening phase is evident either within the grains or on the tilted grain boundary indicated by "A".

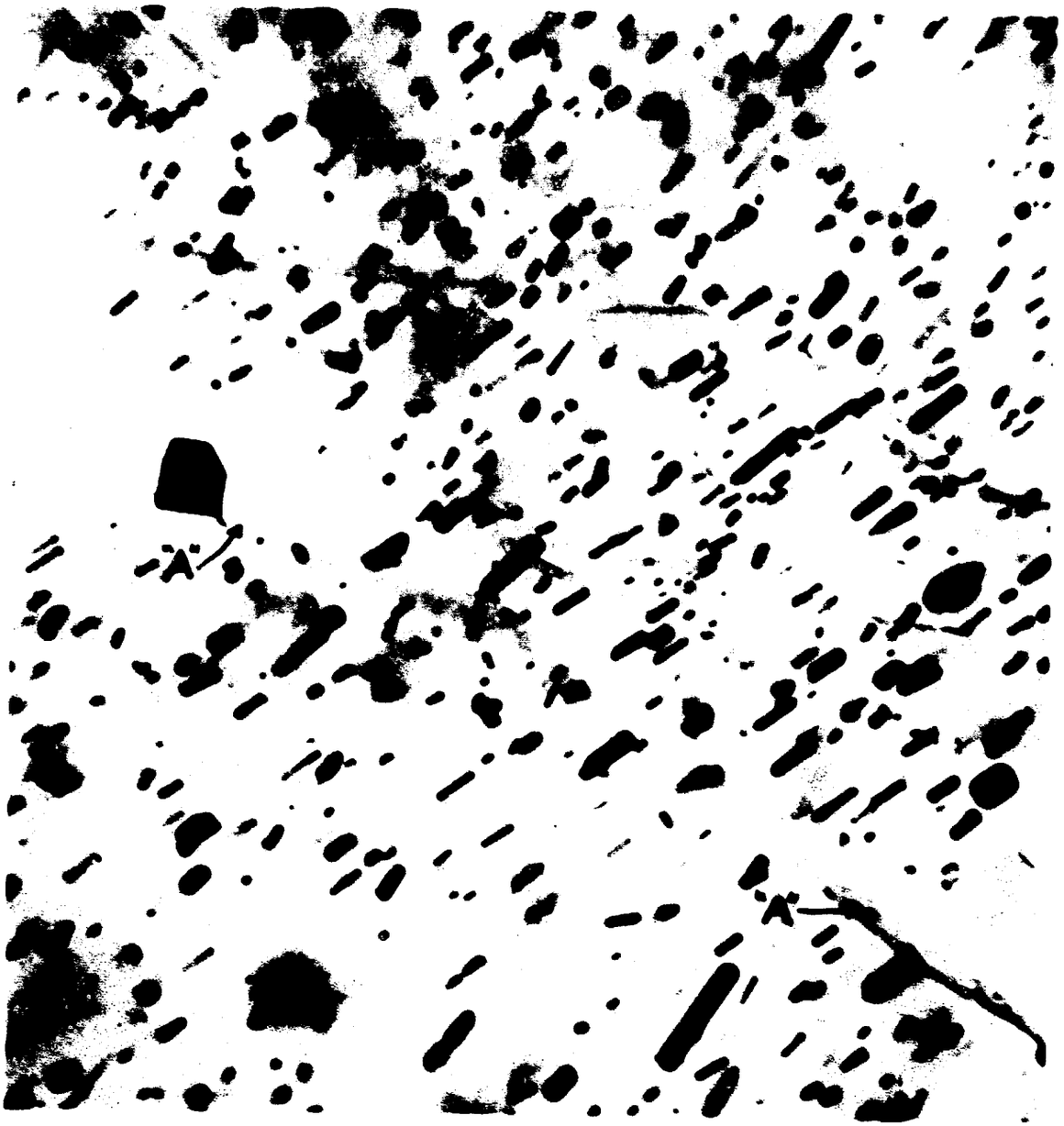

S-NO. 306964

Mag. 20,000X

2024-T4 Cold Water Quenched

Figure 1

Figure 2

THIN FOIL TRANSMISSION ELECTRON MICROGRAPH
OF BOILING WATER QUENCHED 2024-T4 ALLOY

The same numerous particles of dispersoid present in the cold water quenched 2024-T4 alloy illustrated in Figure 1 are also present in this alloy. In addition, particles of precipitate are present on the three grain boundaries (particles indicated by "A"). Smaller precipitate particles (indicated by "B") are present within the grains; these particles are distinguished from dispersoid particles by their shape and by the evidence of strain associated with them.

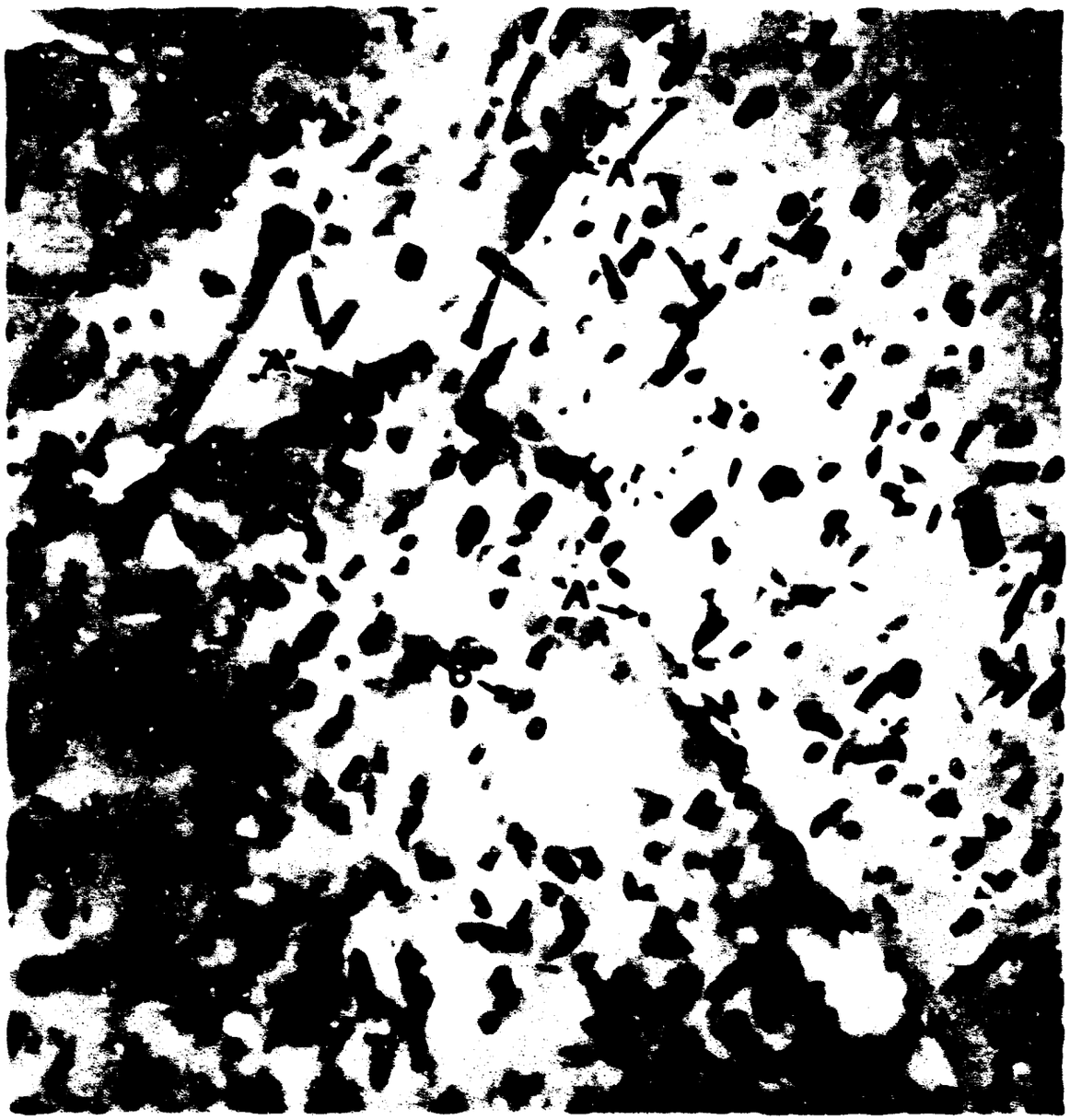

S-NO. 306965 Mag. 20.000X

2024-T4 Boiling Water Quenched

Figure 2

Figure 3

THIN FOIL TRANSMISSION ELECTRON MICROGRAPH
OF COLD WATER QUENCHED 2024-T6 ALLOY

Artificial aging of the cold water quenched 2024-T4 alloy illustrated in Figure 1 to the -T6 temper has resulted in considerable precipitation. Three stages in its development are evident. The precipitate on the tilted grain boundary indicated by "A" is the final, equilibrium form. The Widmanstatten structure within the grains is a transition precipitate. The darker regions within the grains indicated by "B" reflect the presence of zones, the earliest stage of precipitate formation, in which there is clustering of solute atoms only.

S-NO. 306966

Mag. 20,000X

2024-T6 Cold Water Quenched

133/6/TJ

Figure 3

Figure 4

THIN FOIL TRANSMISSION ELECTRON MICROGRAPH
OF BOILING WATER QUENCHED 2024-T6 ALLOY

All features of the cold water quenched 2024-T6 alloy illustrated in Figure 3 are evident:

(1) equilibrium precipitate is present on each of the four grain boundaries, as indicated by "A";
(2) transition phase precipitate again forms the Widmanstatten structure within the grains; and
(3) zones indicated by "B" are present. At the same time, precipitation is more advanced on the grain boundaries. There is alsc some evidence of depletion of zones and transition precipitate in regions adjacent to the grain boundaries, as indicated by "C".

S-NO. 306967

Mag. 20,000X

2024-T6 Boiling Water Quenched

Figure 4

Figure 5

THIN FOIL TRANSMISSION ELECTRON MICROGRAPH
OF COLD WATER QUENCHED 7075-W ALLOY

A small amount of precipitate is evident on the slightly tilted grain boundary, as indicated by "A". This precipitate is not present in sheet or thinner products that are quenched more rapidly. The numerous, larger particles within the grain are dispersoid of an Al-Mg-Cr phase.

S-NO. 306962

Mag. 20,000X

7075-W Cold Water Quenched

Figure 5

Figure 6

THIN FOIL TRANSMISSION ELECTRON MICROGRAPH
OF COLD WATER QUENCHED 7075-T6 ALLOY

The same numerous particles of dispersoid present in the cold water quenched 7075-W alloy illustrated in Figure 5 are also present in this alloy. At the same time, the precipitate (indicated by "A") on the grain boundary is somewhat larger and there is more of it. There is evidence of zone formation as indicated at "B"; however, the zones are relatively small and not clearly resolved at this magnification.

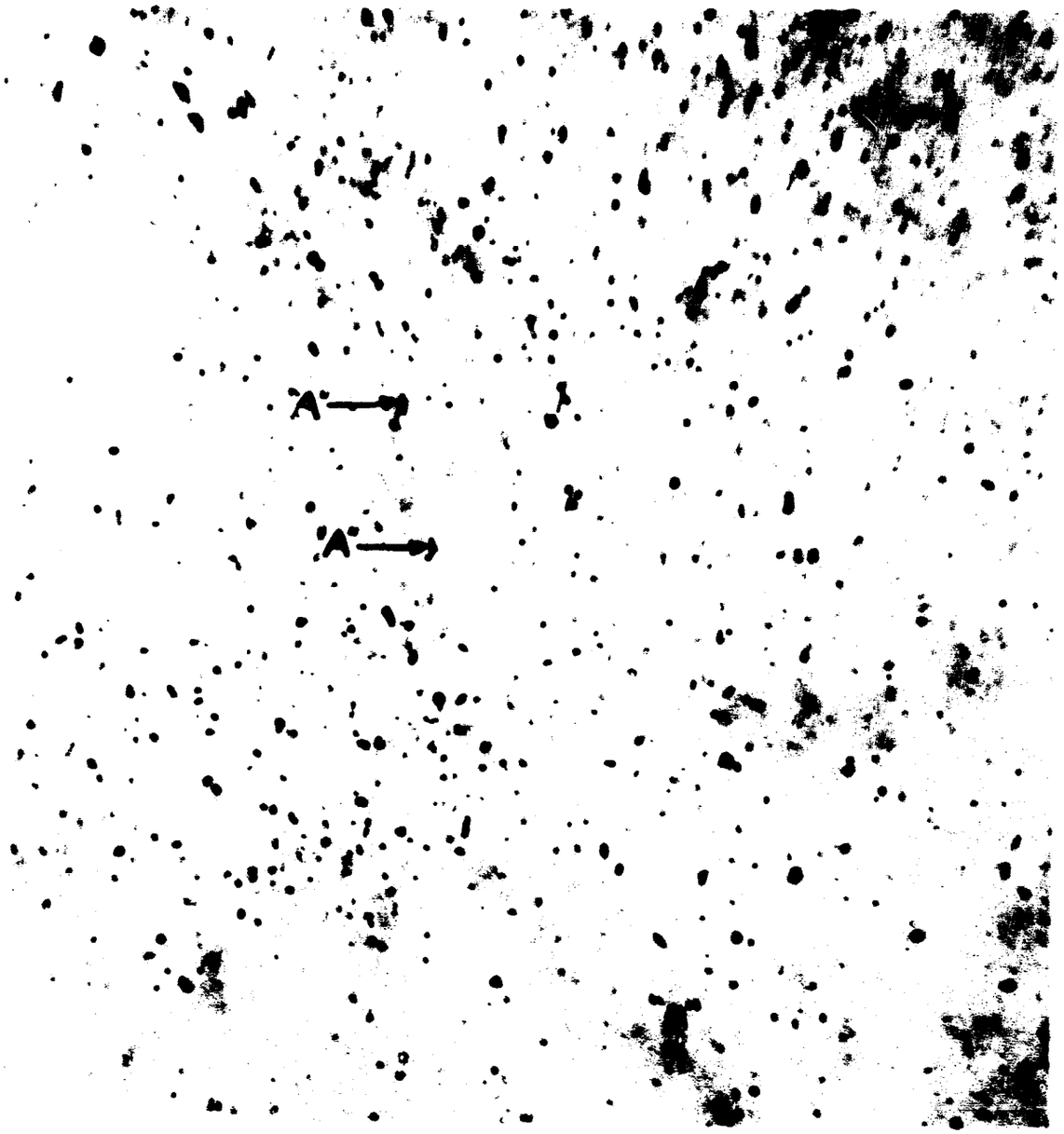

S-NO. 306903

Mag. 20.000X

7075-T6 Cold Water Quenched

Figure 6

Figure 7

THIN FOIL TRANSMISSION ELECTRON MICROGRAPH
OF COLD WATER QUENCHED 7075-T73 ALLOY

As compared to the cold water quenched 7075-T6 alloy illustrated in Figure 6, this alloy contains larger precipitate particles on the grain boundary as indicated by "A". In addition, zones are much more fully developed; they are evident as small dots throughout the grains.

S-NO. 306905

Mag. 20.000X

7075-T73 Cold Water Quenched

Figure 7

Figure 8

THIN FOIL TRANSMISSION ELECTRON MICROGRAPH
OF BOILING WATER QUENCHED 7075-W

As compared to the cold water quenched 7075-W alloy illustrated in Figure 6, this alloy shows a considerable amount of precipitate within the grains as indicated by "A". The light spots such as that indicated at "B" are locations where constituent particles have been removed from the grain boundary during preparation of the specimen.

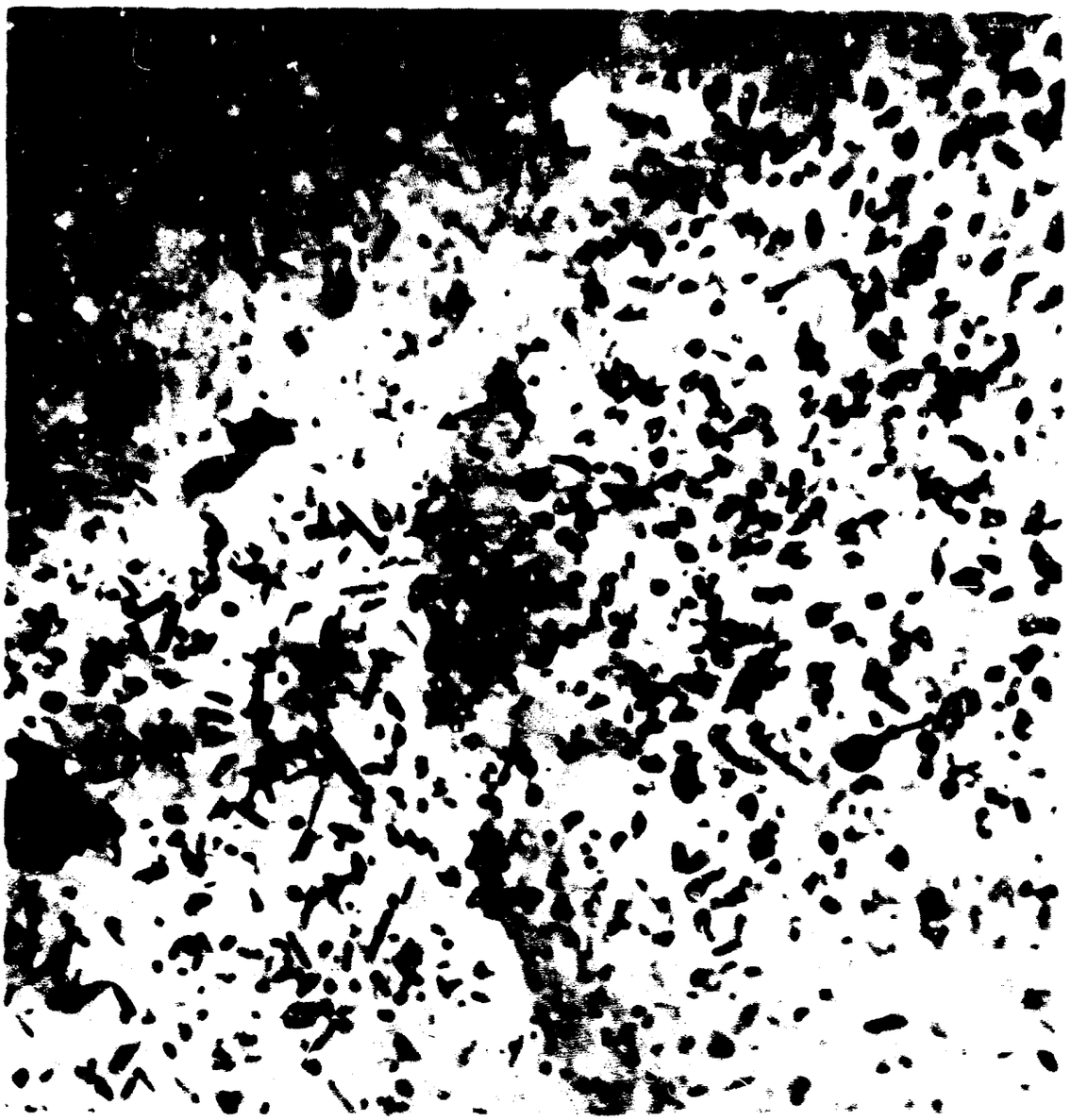

S-NO. 306963

Mag. 20,000X

7075-W Boiling Water Quenched

Figure 8

Figure 9

THIN FOIL TRANSMISSION ELECTRON MICROGRAPH
OF BOILING WATER QUENCHED 7075-T6

The same coarse precipitate seen in boiling water quenched 7075-W alloy illustrated in Figure 8 is also present in this alloy. In addition, fine grain boundary precipitate indicated by "A" has formed. There is some evidence of zone formation, but as was the case for cold water quenched 7075-T6 alloy, the zones are not sufficiently large to be clearly resolved at this magnification. The light spots indicated by "B" are locations where constituent particles have been removed during preparation of the specimen.

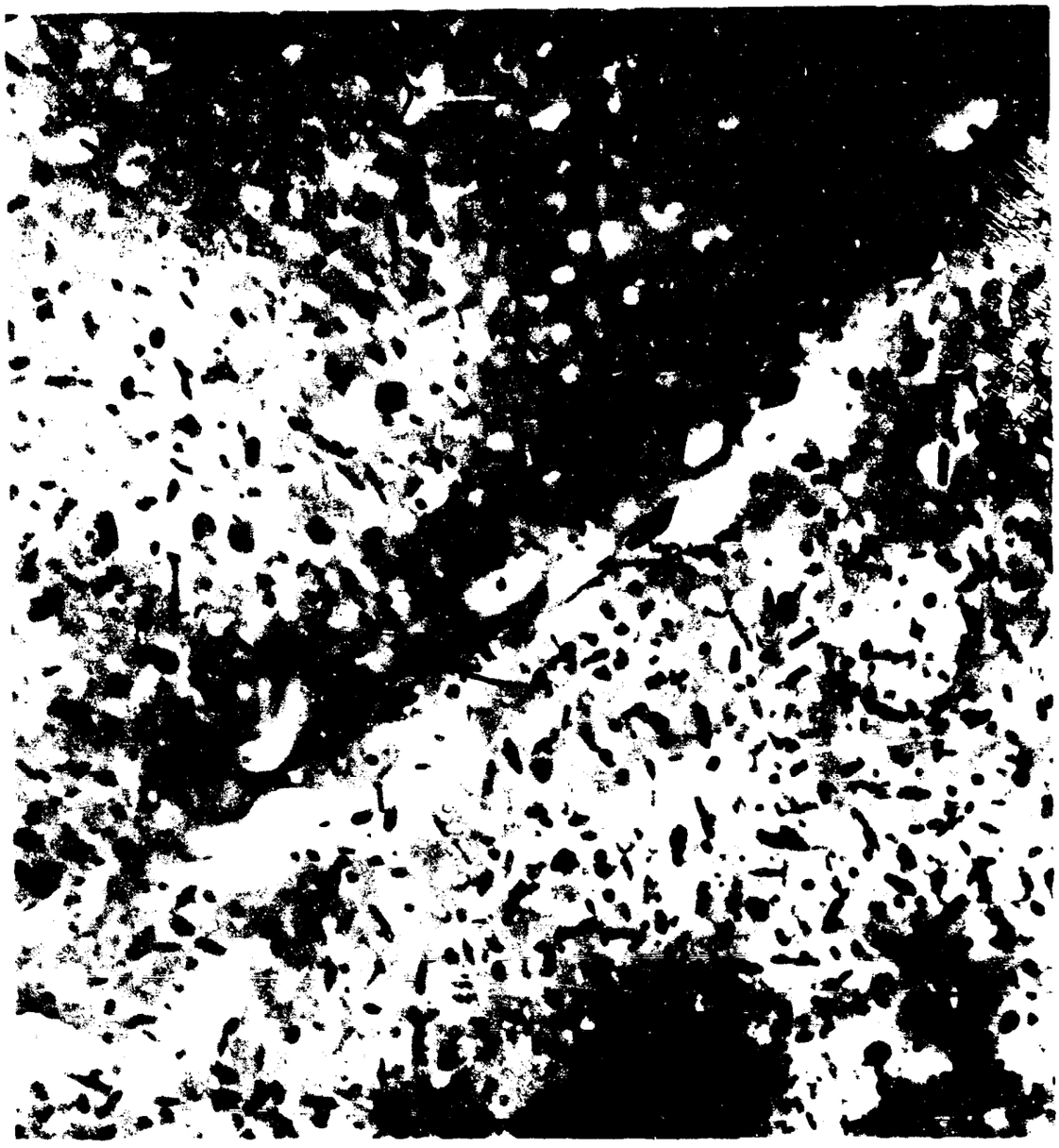

S-NO. 306904

Mag. 20,000

7075-T6 Boiling Water Quenched

133/8/63

Figure 9

Figure 10

THIN FOIL TRANSMISSION ELECTRON MICROGRAPH
OF BOILING WATER QUENCHED 7075-T73

As compared to the boiling water quenched 7075-T6 alloy illustrated in Figure 9, this alloy shows further growth of grain boundary precipitate indicated by "A". In addition, the zones, evident as the numerous fine dots throughout the grains, are more fully developed. The light spots indicated by "B" again are locations where constituent particles have been removed during preparation of the specimen.

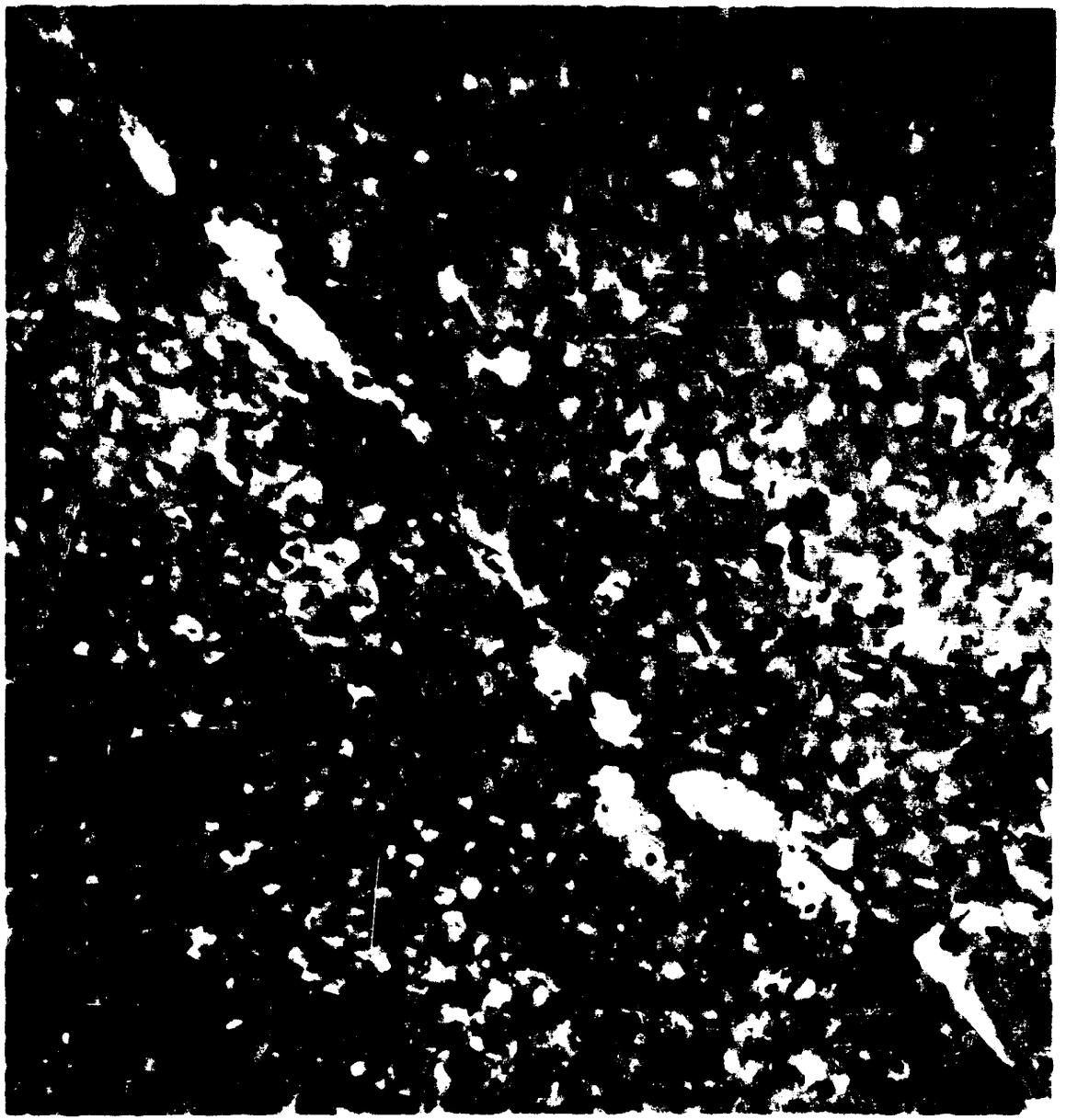

S-NO. 306906 Mag. 20,000X

7075-T73 Boiling Water Quenched

133/10/43

Figure 10

Figure 11

Structure of 2024 as revealed by light microscope. Longitudinal sections from 1/4-inch plate etched in Keller's etch. Mag. 500X.

a

2024-T4 cold water quenched
S.No. 306964

b

2024-T4 boiling water quenched
S.No. 306965

c

2024-T6 cold water quenched
S.No. 306966

d

2024-T6 boiling water quenched
S.No. 306967

a b

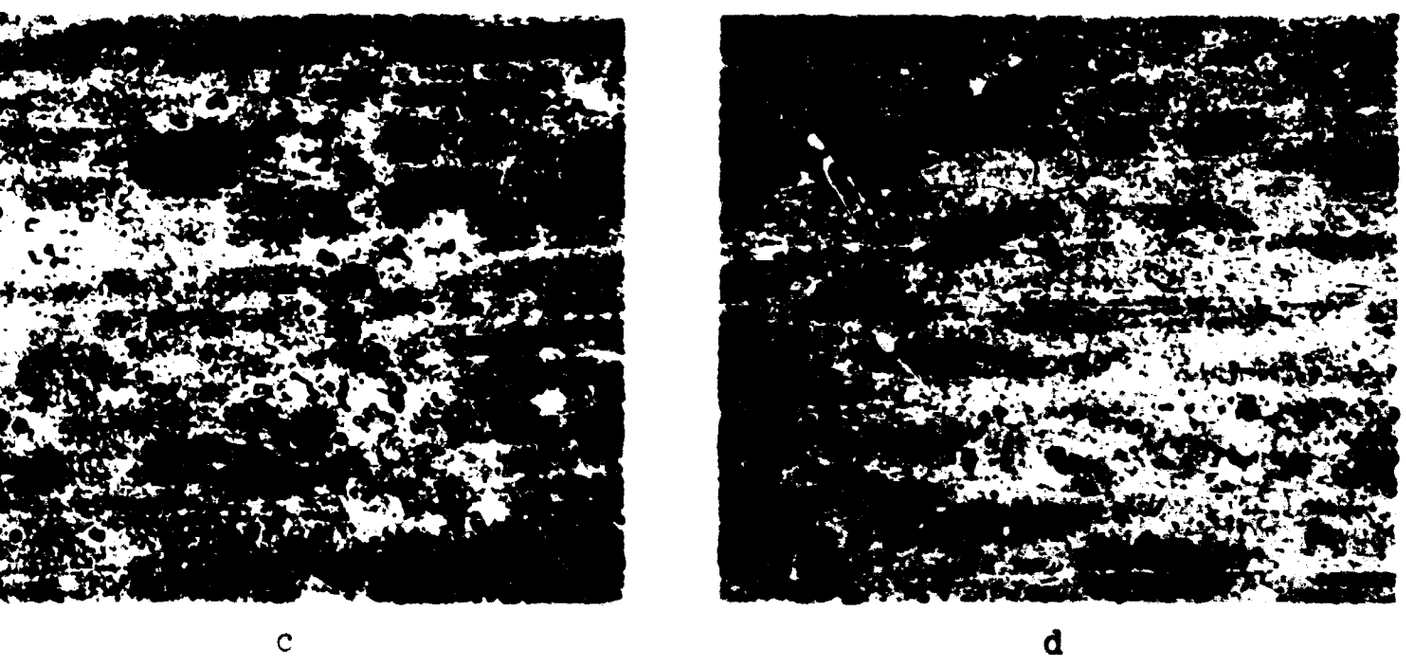

c d

Figure 11

Figure 12

Structure of 7075 as revealed by light microscope.
Longitudinal sections from 1/4-inch plate etched
in Keller's etch. Mag. 500X.

a

7075-W cold water quenched
S.No. 306962

d

7075-W boiling water quenched
S.No. 306963

b

7075-T6 cold water quenched
S.No. 306903

e

7075-T6 boiling water quenched
S.No. 306904

c

7075-T73 cold water quenched
S.No. 306905

f

7075-T73 boiling water quenched
S.No. 306906

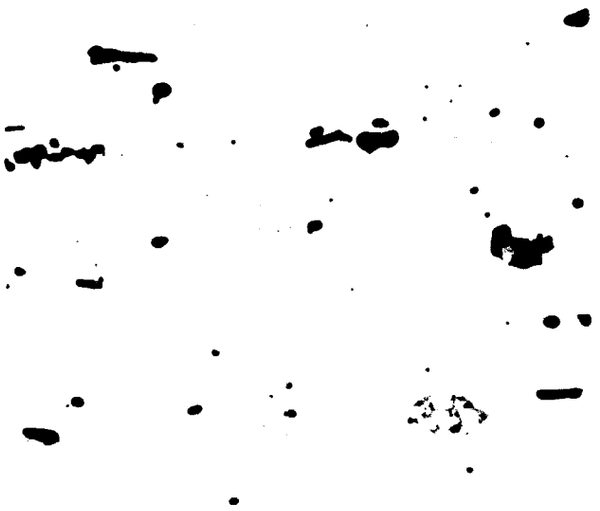

a

d

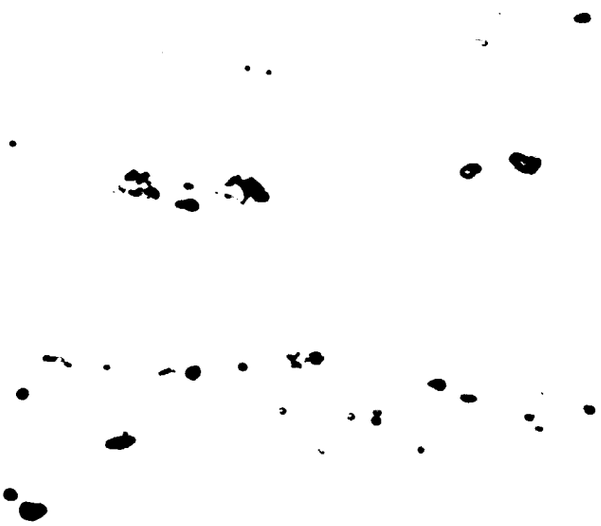

b

e

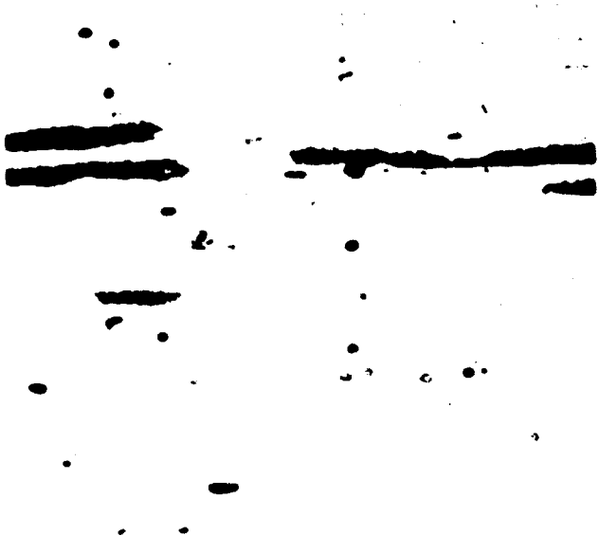

c

f

Figure 12

Figure 13

Magnetic susceptibility versus electrical conductivity demonstrating the proportionality of the two measurements in following solid solution decomposition.

Figure 13

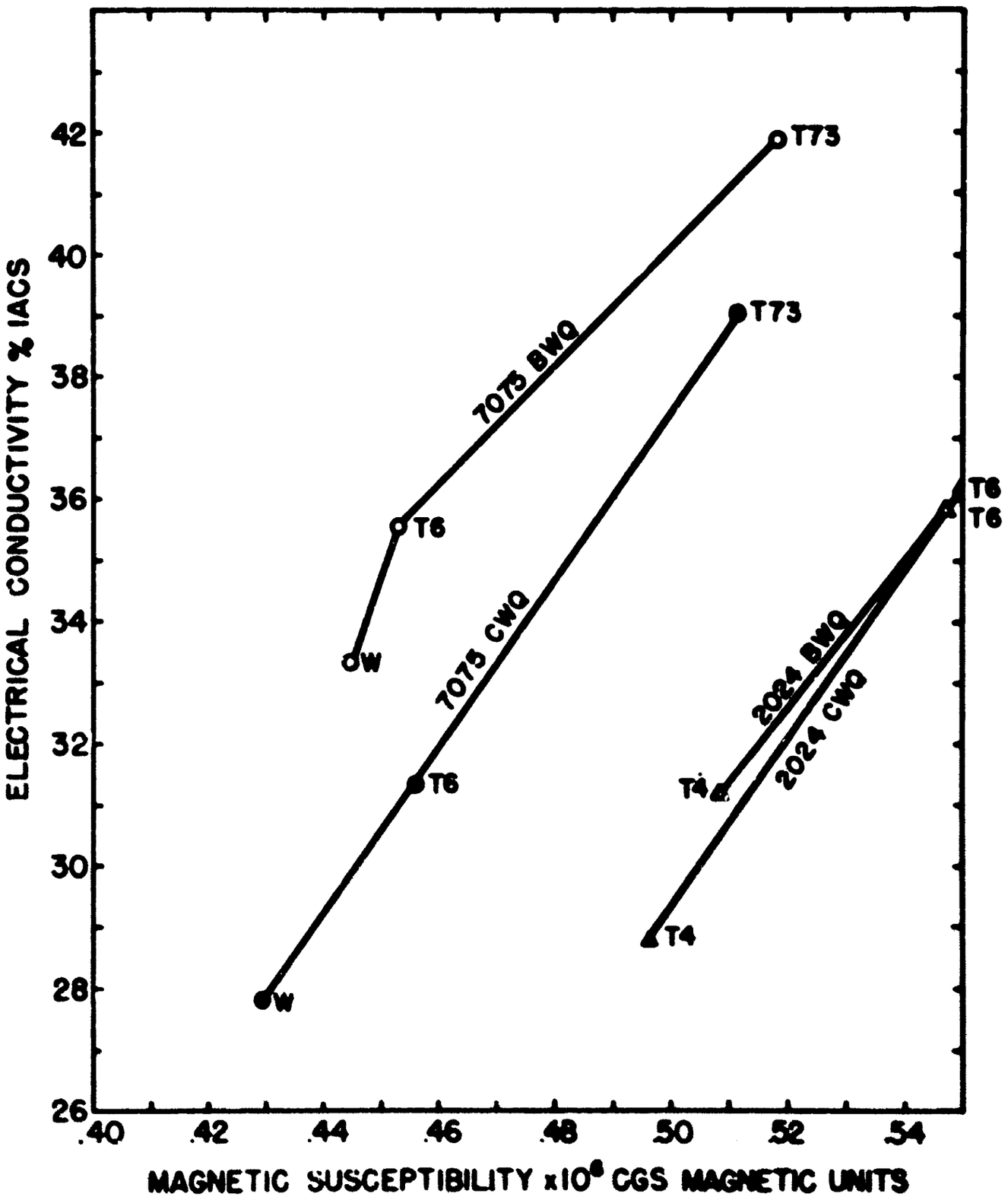
ELECTRICAL CONDUCTIVITY % IACS
MAGNETIC SUSCEPTIBILITY x10⁶ CGS MAGNETIC UNITS
42
40
38
36
34
32
30
28
26
.40
.42
.44
.46
.48
.50
.52
.54
T73
7075 BWQ
T6
W
T73
7075 CWQ
T6
W
T6
T6
2024 BWQ
T4
2024 CWQ
T4

Figure 14

Anodic polarization curves for 2024-T4 and -T6.

Electrolyte	1 N NaCl, pH 4.0
Pretreatment	20 minutes at 10 milliamperes per square centimeter.
Scanning Rate	200 millivolts per minute negative direction.

Figure 14

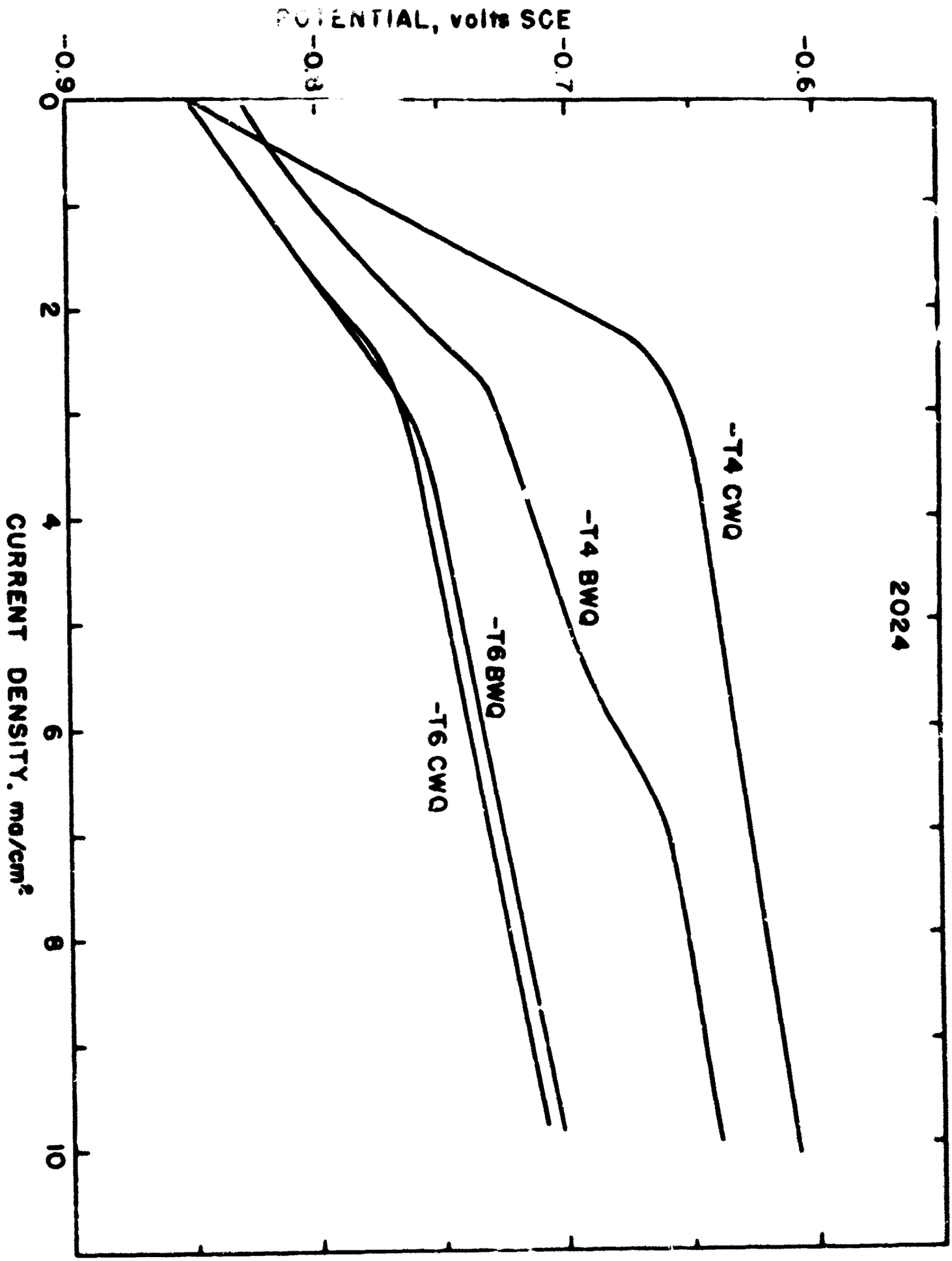
POTENTIAL, volts SCE
-0.9
-0.8
-0.7
-0.6
0
2
4
6
8
10
CURRENT DENSITY, ma/cm²
-T4 CWQ
-T4 BWQ
-T6 BWQ
-T6 CWQ
2024

Figure 15

Anodic polarization curves for cold water quenched 7075.

Electrolyte	1 N NaCl, pH 4.0
Pretreatment	20 minutes at 10 milliamperes per square centimeter.
Scanning Rate	200 millivolts per minute positive direction.

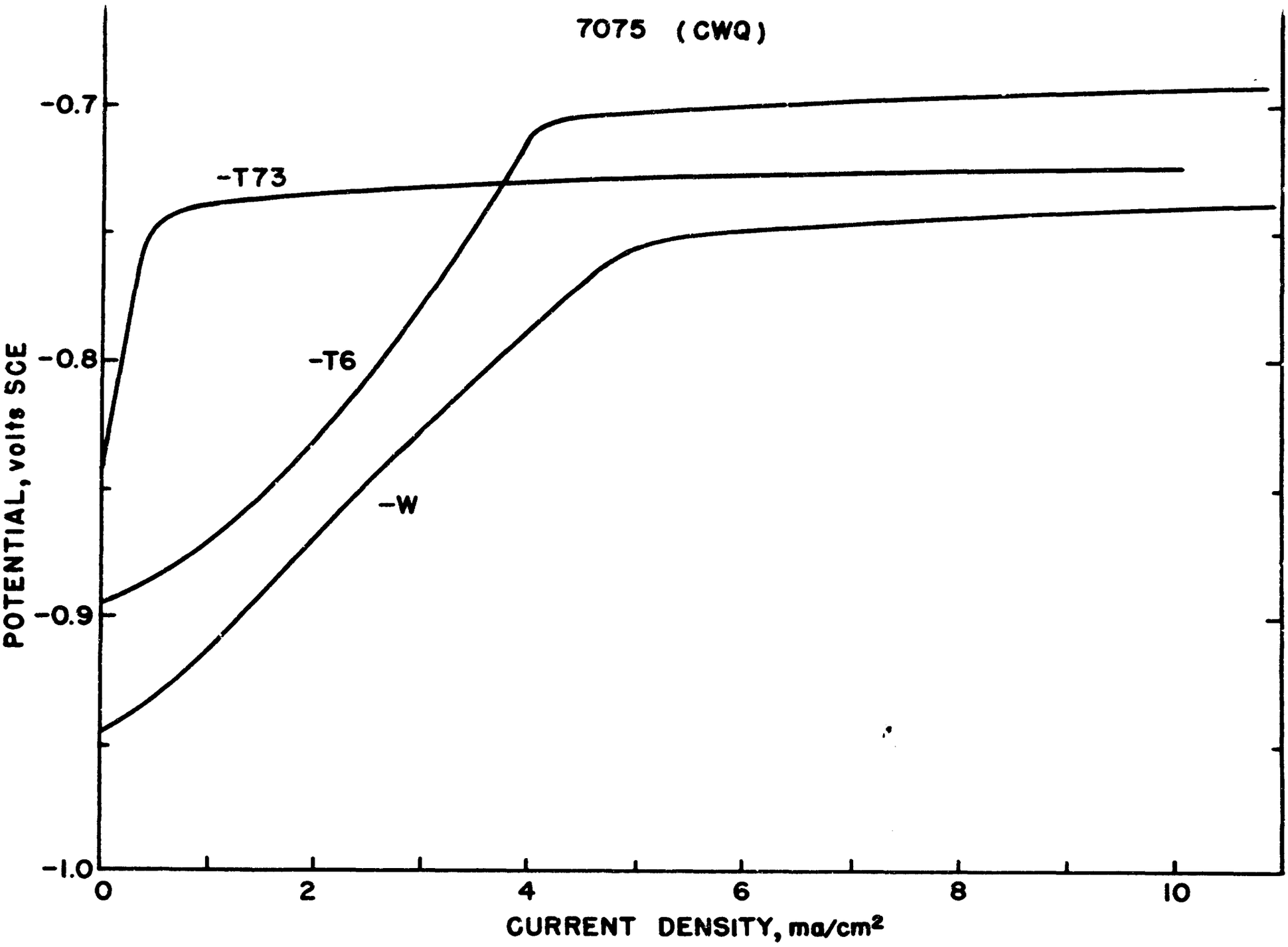
7075 (CWQ)
-0.7
-0.8
-0.9
-1.0
POTENTIAL, volts SCE
-T73
-T6
-W
0
2
4
6
8
10
CURRENT DENSITY, ma/cm²

Figure 16

Anodic polarization curves for boiling water quenched 7075.

Electrolyte	1 N NaCl, pH 4.0
Pretreatment	20 minutes at 10 milliamperes per square centimeter.
Scanning Rate	200 millivolts per minute positive direction.

Figure 16